

PERIODICO di MINERALOGIA
established in 1930

*An International Journal of
MINERALOGY, CRYSTALLOGRAPHY, GEOCHEMISTRY,
ORE DEPOSITS, PETROLOGY, VOLCANOLOGY
and applied topics on Environment, Archaeometry and Cultural Heritage*

^{39}Ar - ^{40}Ar geochronology of mono- and polymetamorphic basement rocks

Igor M. Villa

Institut für Geologie, Universität Bern, Baltzerstrasse 3, 3012 Bern, Switzerland
Centro Universitario Datazioni e Archeometria, Università di Milano Bicocca,
P.za della Scienza 4, 20126 Milano, Italy
igor.villa@geo.unibe.ch

Abstract

The ^{39}Ar - ^{40}Ar technique is often used to date the metamorphic evolution of basement rocks. The present review article examines systematic aspects of the K-Ar decay system in different mineral chronometers frequently found in mono- and polymetamorphic basements (amphibole, biotite, muscovite/phengite, K-feldspar). A key observation is that the measured dissolution rate of silicates in aqueous fluids is many orders of magnitude faster, and has a much lower activation energy, than the rate of Fickian diffusion of Ar. The effects of this inequality are patchy age zonations, very much like those observed in many U-Pb chronometers, unaccompanied by intra-crystalline bell-shaped Ar loss profiles. Recognizing the importance of the respective rates in field situations leads to re-evaluating the ages and the interpretive paradigms in classic examples such as the Central Alpine “Lepontine” amphibolite facies event and the Western Alpine eclogitic event.

Key words: ^{39}Ar - ^{40}Ar dating; diffusion; geochronology; eclogite dating; Lepontine event.

Introduction

As geological systems are exceedingly complicated, it is unavoidable that a few researchers resort to Occam’s Razor: the hypothesis that makes the smallest number of ad-hoc assumptions is worthiest of becoming a working hypothesis that needs to be repeatedly tested following Popperian epistemology. As human mind is exceedingly simple, it is unavoidable that many researchers instead

resort to Confucian imitation: if it is printed, it is necessarily true, and any working hypothesis takes on an immortal life of its own, regardless of prior or subsequent contrary observations. From a short-term, career-oriented viewpoint Confucian imitation is the winning strategy, as it saves the time that a Popperist would waste by constantly verifying/falsifying hypotheses.

The difference between inductive and deductive (respectively “scientific” and “religious” in the modern sense) approaches has permeated

European philosophy for centuries. Aristotle favoured an inductive approach, whereby observations of nature were distilled into an empirical formulation of natural laws capable of accounting for the observed regularities. Plato's approach was the opposite, as it assumed that laws exist in an ideal, transcendent realm, which philosophers deduce from theoretical reasoning.

One of the dangers of an undue combination of inductive and deductive approaches, when associated with incomplete observation datasets, is that a preliminary working hypothesis (a legitimate, albeit partial, result of empirical Aristotelian induction) is elevated into the Platonic realm of immutable laws. Popperian verification/falsification is no longer conceivable, and observations are deduced (and, if necessary, filtered and twisted) from the laws.

The case of geochronology of metamorphic basement rocks illustrates how conceptions became misconceptions and how recent additional observations can restore credibility to the field of quantitative geology. In the 1960s geochronologists observed that isotopic ages did not always record the first formation of minerals. Especially in metamorphic rocks, mineral ages were younger than expected. The first attempts to rationalize the discordant ages of zircon samples (Tilton, 1960; Wetherill, 1963) assumed that Fickian diffusion of Pb was the one and only cause of age discordance. Tilton (1960, Figure 3) quantified the diffusion coefficient of Pb in zircon and calculated that the discordant Proterozoic samples of his study recorded Pb loss with $D/a^2 = 25 \times 10^{-12} \text{ a}^{-1} = 8 \times 10^{-19} \text{ s}^{-1}$. Wetherill (1963) proposed a sophisticated mathematical model (with interesting typographic errors in the subtitle and in his Figure 5, sample 150) to predict a zircon's discordance as a function of differential diffusion of U and Pb.

Hart (1964) then exported the view of purely diffusive loss of Pb from zircon to other minerals. In the contact aureole of the Eocene Eldora pluton he observed that the ages of

minerals in the pluton's country rocks were rejuvenated. He attributed the loss of Ar and Sr to diffusion, despite the knowledge provided by petrology (skarns consist of low- P , high- T mineral assemblages formed by fluid-associated mass transfer in a chemically open system) and ore geology (porphyry copper deposits are found near the apex of a granitoid body because chalcophile elements are transported by fluids exsolved from the pluton, not because heat creates copper), and went on to calculate Ar diffusivity coefficients for biotite; a reassessment of the validity of his conclusions follows below. This extreme diffusionism was sufficiently simple for a large part of the users' community, and Dodson (1973) systematized the approach by mathematically defining the "closure temperature" T_c for the retention of Ar, Sr, Pb, etc., in a cooling system. The closure temperature would be a useful concept if the retention of radiogenic isotopes only depended on T , as is the case for retention of fission tracks and He in apatite. Only in this case cooling histories could be constrained and, to the extent that the paleo-geothermal gradient is accurately known, provide a proxy for exhumation. As an example, the "closure temperature" of a 100 μm radius phlogopite grain cooling at 20 $^\circ\text{C}/\text{Ma}$ can be calculated from the diffusivity measurements by Giletti (1974) as $T_c = 404$ $^\circ\text{C}$. However, misinterpretations arise whenever one of the initial assumptions is incorrect.

The first data-set that did achieve a limited measure of belief revision was the combination of U-Pb ages by secondary ion microprobe with cathodoluminescence imaging by Gebauer et al. (1988). These workers documented that discordant zircon grains consist of core-rim zones that are individually concordant and reflect discrete crystal growth/reaction events; discordance solely results from the mixing of concordant crystal zones, not from Pb diffusion out of a single, inert, homogeneous zircon matrix. This observation has been universally

reproduced, and the present-day consensus of all but a few U-Pb geochronologists is that zircon imaging by cathodoluminescence is the key to an accurate interpretation of petrogenesis, and therefore of ages. In a large proportion of samples of metamorphic minerals studied in sufficient detail it is observed that ages are not constant across individual grains. A very simple yet very rigorous distinction is provided by the mathematical form taken by the intra-grain age variations. Whenever diffusion has occurred in a homogeneous matrix, the concentration of the diffusant as a function of distance obeys a bell-shaped curve (the so-called error function,

or erf), whereby the matrix remains inert by definition. The observation of patchy textures, on the other hand, can only be reconciled by fluid-assisted (neo-/re-)crystallization. The main question is what process has the fastest rate. One can compare the experimental determinations of the diffusion rate in phlogopite (Giletti, 1974) with the dissolution/precipitation rate in silicates at large (Wood and Walther, 1983). Moreover, Villa (2010) has re-evaluated the original Giletti (1974) tables and found that the data overestimate true Ar diffusivity; this makes the present argument even stronger. The comparison is displayed in Figure 1. It is

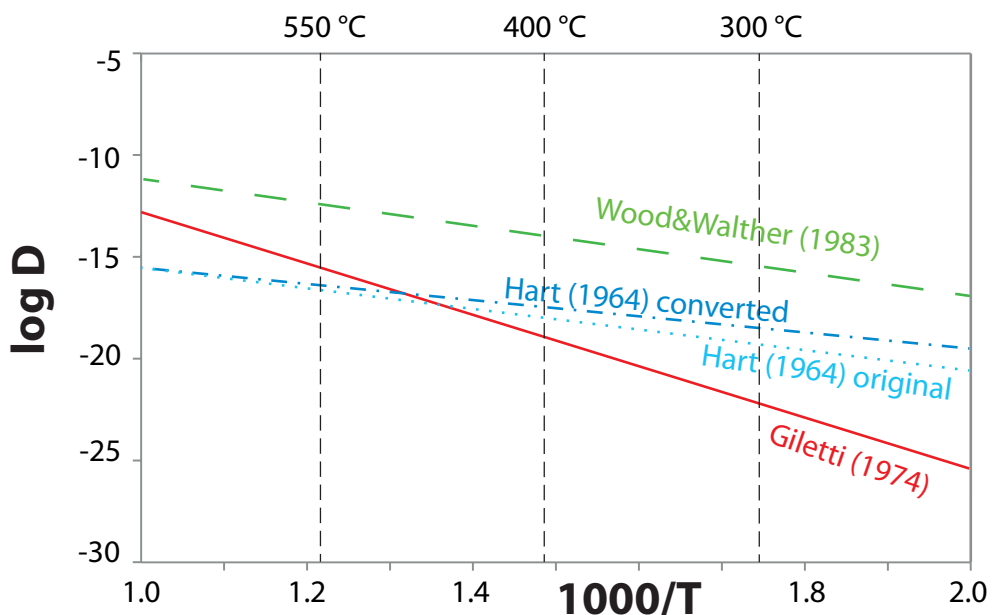


Figure 1. Arrhenius diagram comparing different Ar degassing rates. The lines are labelled with the relevant references. The dissolution rate obtained experimentally by Wood and Walther (1983) is equivalent to an Ar degassing rate, as a dissolved mineral is completely outgassed. The Ar loss rates calculated by Hart (1964) for biotite in the Eldora contact aureole are shown as a dotted line. The dash-dotted line is a recalculation of Hart's (1964) original data after correction for grainsize. A comparison with the other two biotite Ar loss rates strongly suggests that Hart's samples were dominated by Wood-Walther dissolution, not by diffusive loss. It also must be kept in mind that the Giletti (1974) Ar loss rates overestimate diffusion (Villa, 2010).

noteworthy that for $T = 350\text{ }^{\circ}\text{C}$ the dissolution rate k of a $100\text{ }\mu\text{m}$ grain is almost 10^3 times faster than diffusion, with implications for field estimates that will be reviewed below. This explains the universal observation (Villa and Williams, 2013, and references therein) that patchy recrystallization textures associated to patchy intra-grain age variations are ubiquitous in metamorphic minerals, whilst genuine bell-shaped age gradients required by diffusion theory are extremely rare exceptions. When diffusion is superposed on recrystallization, the steepest age gradient found in a sample represents the upper limit for diffusivity.

Villa and Williams (2013) also imply that “water is water is water”: the water molecule does not know whether the modifications of shape and composition of a mineral it is causing will be labelled “metamorphism” by Greek-speaking geologists or “alteration” by Latin-speaking ones. In general terms, metamorphism, metasomatism and alteration are three manifestations of the same process driving the crystallization of metamorphic phase assemblages, *viz.* dissolution/reprecipitation (Putnis and Austrheim, 2013). The essential perception of metamorphic processes has shifted in most of the petrological community, even if not all Earth scientists have become aware of it. The consensus has now been reached that all paragenetic changes, both prograde and retrograde, require aqueous fluids (Jamtveit, 2010).

This projects the dissolution rates measured by Wood and Walther (1983) to the forefront of any quantitative estimate of metamorphism. It is therefore of special importance that no subsequent studies have revised downwards the dissolution rate proposed by Wood and Walther (1983). Therefore, it is legitimate and meaningful to compare the relative importance of Ar loss by volume diffusion and by dissolution/reprecipitation in geologically realistic situations. The rate of Ar loss from biotite published by Hart (1964) for the Eldora

aureole is shown in Figure 1 together with the dissolution rate measured by Wood and Walther (1983) and the nominal Ar diffusivity measured by Giletti (1974). The Eldora samples lie a few orders of magnitude above Giletti’s (1974) experimental data, close to the Wood-Walther line. This rounds off the proof that the mechanism causing the biotite age trend in the Eldora aureole was not heating but fluid-induced recrystallization.

Geochronology of metamorphic amphiboles

The amphibole family is comprised of tens of compositionally different varieties, many of which are index minerals of a specific metamorphic facies. Many rocks contain several generations of heterochemical amphiboles. This is an effect of the great stability of amphibole, which is seldom completely consumed during subsequent prograde or retrograde metamorphic reactions.

The Ar diffusivity in hornblende was most recently reassessed by Villa et al. (1996). These authors noticed a few inconsistencies in the older literature, and proceeded to a recalculation both from a reevaluation of literature data and from new data obtained using several complementary analytical techniques (stepwise heating, stepwise leaching, and laser microprobe with infrared and ultraviolet laser beams, piston-cylinder heating).

The corrected diffusion coefficient and activation energy are $\log D_0 = -2.68$ and 64.6 kJ/mol , respectively (Villa et al., 1996, p. 79); these values translate to a Dodsonian “closure temperature” of $620\text{ }^{\circ}\text{C}$ for a $100\text{ }\mu\text{m}$ radius grain cooling at $20\text{ }^{\circ}\text{C/Ma}$. This high retentivity ensures that most amphibolite-facies amphiboles record the age of their own growth, or extremely close to it.

In the process of maximizing the information derived from ^{39}Ar - ^{40}Ar analyses, Villa et al. (1996) artificially mixed different minerals,

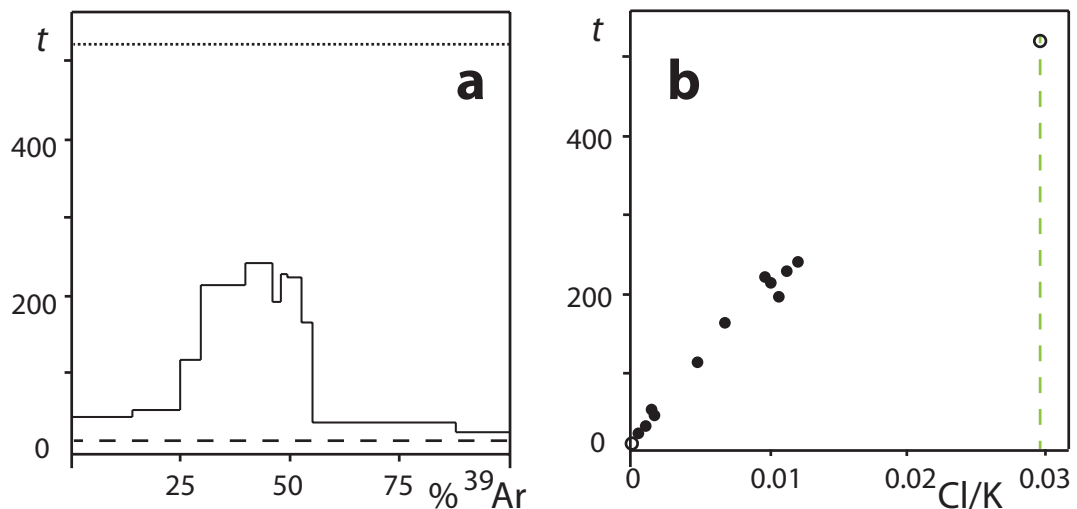


Figure 2. Systematics of mixing different mineral phases, modified after Villa et al. (1996). (a) Age spectra of amphibole MMhb1 (dotted line), of K-feldspar GA-1 (dashed line) and of the artificial amphibole-feldspar mixture (solid line). The age spectrum alone allows no clear recognition of the two end-members. (b) Common-denominator three-isotope correlation diagram with $x = \text{Cl/K}$ (from $^{38}\text{Ar}_{\text{Cl}}/^{39}\text{Ar}_{\text{K}}$), $y = \text{age}$ (from $^{40}\text{Ar}_{\text{rad}}/^{39}\text{Ar}_{\text{K}}$). The Kfs is practically Cl-free (Smith, 1974) and has an age of ca. 18 Ma, the amphibole has an age of ca. 520 Ma and a Cl/K ratio of ca. 0.029. The individual heating steps plot along the line connecting the two pure end-members. If the Cl/K ratios are known (e.g. from electron probe microanalyses) then the ages of the end-members are unambiguously constrained.

and then deconvolved the mixture using common-denominator three-isotope correlation (CDTIC) diagrams, establishing the validity of the approach from the known chemical compositions and ages of the pure starting materials (Figure 2). This task was made easy by the fact that amphiboles usually contain comparatively high concentrations of Ca, Cl and K, which all produce an Ar isotope when irradiated. The five Ar isotopes allow a linear decomposition into five components (Ar deriving from Ca, Cl and K; trapped Ar; radiogenic Ar), which can be plotted as ratios defining the axes of a 4-dimensional point distribution (e.g. Villa, 2001). If ratios having a common denominator are chosen as axes of the 4-dimensional space, any 2-dimensional projection of the point distribution gives rise

to a CTDIC, which displays the mixing end-members as vertices of the minimum polygon enclosing all points (Villa, 2001).

The compositional variability of amphiboles was exploited by Villa et al. (2000) to constrain the multistage evolution of the Malenco ocean-floor rocks before and during the Alpine orogeny. The petrology, established beforehand, related the oldest amphibole generation, Na-rich Am1, to pre-Alpine high-pressure conditions; Ca-rich Am2 was attributed to an early high-temperature phase of the Alpine orogenic cycle; Am3 replaced Am2 in distinctive reaction patches as metamorphic grade decreased to lower amphibolite facies. Other samples in the area (not studied by Villa et al., 2000) record the formation of greenschist-facies actinolitic Am4. Correspondingly, the CDTIC diagrams revealed

that (1) correlations were clearly recognized; the relative abundances of three amphibole generations in different samples were well distinguishable; (2) the successive formation of each generation (at temperatures always lower than the “closure temperature” for Ar loss) was reliably dated. This allowed dating the double P-T loop recorded by the Malenco metabasic rocks (Villa et al., 2000, Figure 9).

Geochronology of monometamorphic micas

As the geochronometric systematics of micas has often been misunderstood, it is didactically most fruitful to begin the discussion with an example of rocks recording a geological evolution as simple and as recent as possible. The Lepontine Dome in the Central Alps, consisting of polymetamorphic gneisses and monometamorphic Mesozoic sediments, has been the object of a large number of papers, which came to very contrasting conclusions regarding the age of Alpine metamorphism (e.g. Allaz et al., 2011, and references therein). As pointed out by Villa (1998, Figure 1), in the idealized case of a monotonic regional distribution of mineral ages decreasing as a function of distance from a high grade metamorphic core, there is an inverse relationship between the estimated age of the metamorphic peak and the estimated “closure temperatures” of these minerals. Mineral chronometers far from the core, outside (down-temperature) of their “closure isograd”, record mixed ages that exceed the age of the metamorphic peak due to isotope inheritance. Mineral chronometers near the core experienced temperatures higher than their “closure temperatures” and therefore record “cooling ages” younger than the metamorphic peak. If the metamorphic peak is as old as the oldest mineral ages observed in the field area, most mineral ages of that region are younger than the peak, which means that their “closure isograd” lies far from the core. If the metamorphic peak is as young

as the youngest mineral ages of the field area, then most mineral chronometers record isotope inheritance, which requires that their “closure isograd” is close to the core. Because in such an idealized field situation the “closure isograds” of the different minerals are supposed to be parallel to the concentric metamorphic isograds, the relative sequence of “closure temperatures” is rigidly fixed. Modifying one T_c value for one mineral requires modifying all others. A review of existing diffusionist literature on the Central Alps (a crucial area, as it was here that all the “canonical” calibrations were based) should reveal if this edifice is internally consistent. On the basis of the “closure temperature” approach for mica ages, a simple chain of very rigorous and correctly applied logical implications led Steck and Hunziker (1994, Figure 12) to predict the “closure temperature” of monazite for Pb loss. Their prediction is not based on one single sample but on the regional pattern defined by hundreds of mineral ages obtained up to 1993, which define an approximately bowl-shaped dependence of mineral ages along an E-W traverse across the Central Alps. The focus is on the reproducible relative pattern of muscovite and monazite mineral ages. The observation by Steck and Hunziker (1994, Figure 12) is that it is always true that $t_1 < t_2 < t_3$, where t_1 is the muscovite K-Ar age, t_2 the monazite U-Pb age and t_3 the muscovite Rb-Sr age. Their interpretation further assumes that peak metamorphic conditions were reached 38 Ma ago; as $t_3 < 38$ Ma inside the staurolite isograd, all mineral ages on the high- T side of the staurolite isograd are “cooling ages”. This interpretation had the side-effect of justifying their choice of considering mono- and polymetamorphic mica samples together, as any record of the pre-Alpine history was believed to have been erased. From the inequality governing “cooling ages” it is logically flawless to derive an inequality governing “closure temperatures”: $T_{c1} < T_{c2} < T_{c3}$.

Steck and Hunziker (1994) assumed $T_{c1} = 350^\circ\text{C}$, $T_{c3} = 500^\circ\text{C}$, and derived $T_{c2} \approx 450^\circ\text{C}$. Upward adjustments to T_{c1} or T_{c2} have a domino effect: the relative T_c inequality must be maintained, and all “closure temperatures” increased in parallel. This domino effect is driven to the extreme by the direct determination of Pb diffusivity in monazite (Cherniak et al., 2004), which established that $T_{c2} > 800^\circ\text{C}$. Peak metamorphic temperatures in the Central Alps did not exceed 650°C . This means that all monazite samples record the age of their formation at the metamorphic peak (Janots et al., 2008). Since monazite U-Pb ages are younger than muscovite Rb-Sr ages across the entire Central Alps (Steck and Hunziker, 1994, Figure 12), the latter must have preserved inherited ^{87}Sr even in the highest-grade core area around 650°C . Therefore, the age of the Lepontine event cannot be 38 Ma but must be younger and locally variable (as defined by monazite ages), around 15-25 Ma. This in turn implies that all K-Ar ages > 25 Ma also contain inherited ^{40}Ar , *i.e.*, that they do not record “cooling ages”. Thus, most white mica K-Ar ages in Steck and Hunziker (1994) do not date “cooling below T_c ”; the existence of genuine, inheritance-free “cooling ages” in the polymetamorphic basement gneisses of the Central Alps appears to be exceedingly sporadic in the very original data-set. Subsequent studies (e.g. Tartèse et al., 2011) document a tight parallelism between monazite and white mica ages and attribute it to the overwhelming importance of fluid-assisted recrystallization compared to pure temperature-controlled diffusion.

To exclude isotopic inheritance, ubiquitous in gneisses, Allaz et al. (2011) only studied monometamorphic metasediments from the center of the previously described classic area. In the Piora sector (Central Alps) they obtained thermobarometric data that clearly distinguished between samples recording petrologic disequilibrium (in which the peak

metamorphic paragenesis had been modified by retrograde reactions, in such a way that the reaction equilibria calculated by the TWQ software do not intersect all in the same point in the P-T plane) from equilibrium samples, in which all linearly independent reactions intersect in one point. Age data pertaining to the two classes of samples were compared. It is not surprising that retrogression reactions affect the ages; the novelty of the Allaz et al. (2011) paper lies in the degree of rigor in examining the presence of disequilibria, in the redundancy of the number of envisaged reactions, as well as in the thermodynamic identification of the retrogressed minerals deviating from equilibrium. Focusing on Molare, one of the four areas studied by Allaz et al (2011), it is possible to reconstruct the following segment of the P-T evolution (Figure 3a) by combining the multichronometric data with the petrological findings. The metamorphic peak (840 ± 50 MPa, $594 \pm 14^\circ\text{C}$) was reached *ca.* 18-19 Ma ago, as constrained by the monazite U-Pb ages (Janots et al., 2009). The muscovite ^{39}Ar - ^{40}Ar age of sample AMo0410, 18.9 ± 0.8 Ma, is identical to the monazite age. Exhumation proceeded; nearby sample AMo0409 was formed at lower-grade conditions (660 ± 20 MPa, $573 \pm 11^\circ\text{C}$) at 17.9 ± 0.6 Ma, as dated by muscovite growth. Soon afterwards the paragonite-out boundary was crossed and the first paragonite generation, Prg-1, was mostly consumed. When the rock's P-T-A-X conditions allowed it, Prg-2 grew. The ^{39}Ar - ^{40}Ar age of paragonite AMo0410, 13.3 ± 2.3 Ma, dates the re-entry into the paragonite stability field at *ca.* 380 MPa, 480°C . In contrast, paragonite samples from Frodalera, 5 km NNW of Molare, were not destabilized and their ^{39}Ar - ^{40}Ar ages coincide with the muscovite ages.

The K-Ar age of 16.3 ± 0.4 Ma obtained on the two biotite samples AMo0409 and AMo0410 may initially appear as cooling ages that provide no further insight. Moreover, both samples are slightly chloritized (Allaz et al., 2011, p. 711),

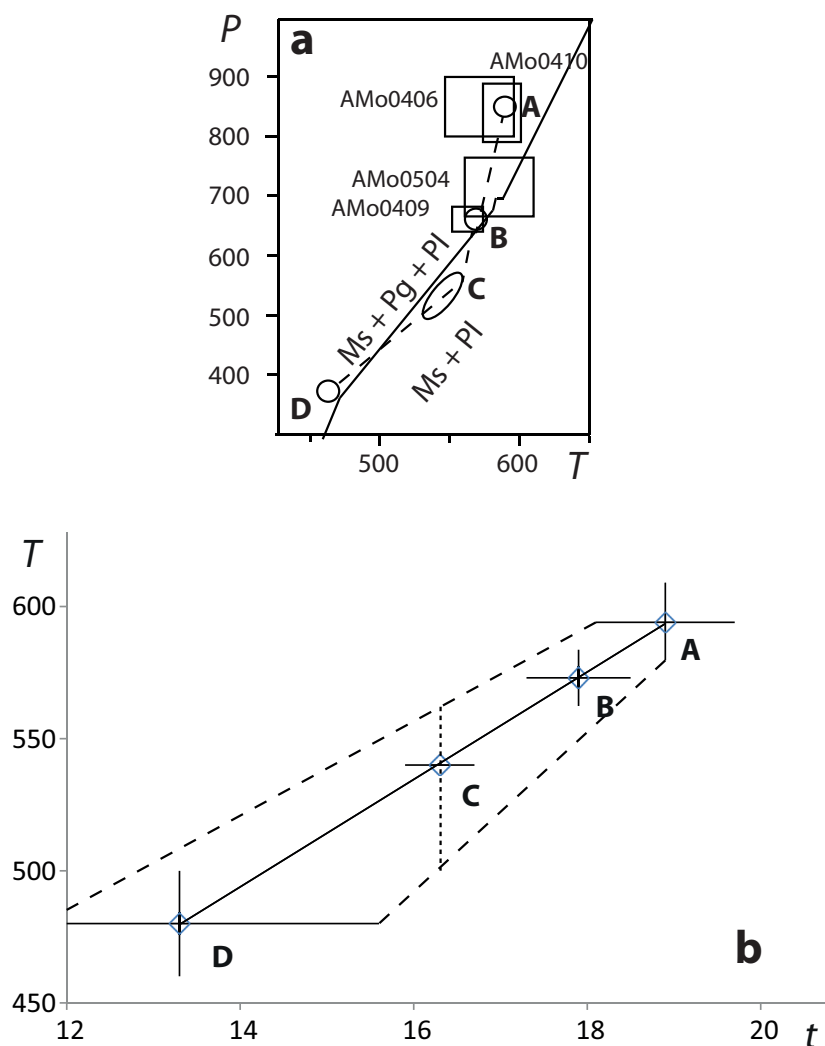


Figure 3. (a) Detail of the phase stability diagram for the four samples from Molare (modified after Allaz et al., 2011). Solid line, paragonite stability boundary. The four squares are the P - T conditions estimated from the respective phase assemblages for the four samples in the Molare area. The dashed line is a schematic representation of the evolution of AMo0410. The ellipses (circles) denote the formation/closure ages of four dated minerals: A, muscovite AMo0410; B, muscovite AMo0409; C, biotite AMo0410; D, paragonite AMo0410. (b) Time-temperature diagram for the four Molare samples. Points A-D are from Figure 3a. Points A, B and D record formation ages. Point C dates the closure of biotite; it is interpolated between B and D, and corresponds to the sum of two resetting mechanisms, chloritization and diffusion. The interpolated temperature of Ar retention (500-560 °C) is thus the lower limit for the purely diffusive “closure temperature”.

which further limits their usefulness. However, the pseudosection diagram of the four Molare samples (Allaz et al., 2011, Figure 11b) does provide very good constraints on their pressure and temperature evolution, from which it is possible to derive an average cooling and exhumation rate between 18.9 and 13.3 Ma. The growth of the Prg-2 generation occurred at 13.3 Ma, $P = 380 \pm 20$ MPa, $T = 480 \pm 20$ °C. This exhumation by 460 MPa in 5.6 Ma corresponds to roughly 3 mm/a. The Molare rocks cooled by ca. 114 °C in the same interval, i.e. by 20 °C/Ma. Around 7 Ma later the rocks reached the apatite fission track retention isograd (Janots et al., 2009), which corresponds to an average cooling rate of ca. 50 °C/Ma between 14 and 7 Ma ago. The most recent exhumation since the Late Miocene slowed down again and resulted in an average cooling rate < 15 °C/Ma.

For AMo0409 and AMo0410 it is possible to interpolate the temperature prevailing at the time of biotite closure, 16.3 ± 0.4 Ma, namely the interval 500-560 °C (Figure 3b). As the biotite is slightly chloritized, this temperature is an underestimate of the true Dodsonian “closure temperature”. Moreover, as the P - T trajectory had to be concave in order to intersect the paragonite stability boundary twice, the temperature prevailing at 16.3 Ma was higher than the linearly interpolated value. It is interesting to note that from this field area one derives an even higher Ar retentivity than that proposed for biotite samples from the Larderello geothermal field (e.g. Villa and Puxeddu, 1994).

Geochronology of polymetamorphic, reheated, retrogressed rocks

The previous examples of monometamorphic rocks recording a monotonic P - T evolution are comparatively exceptional. Most rocks that are in outcrop at the present day are polymetamorphic.

An example illustrating the potential and limitations of ^{39}Ar - ^{40}Ar dating in a

polymetamorphic rock suite is a traverse of the Western Alps (Villa et al., 2014). A strongly simplified geological history features three regimes: a sedimentary oceanic basin was filled with detrital white mica of Hercynian age; the oceanic basin was subducted during the Alpine convergence and eclogitized; the eclogites were sheared in greenschist facies and exhumed to the surface. In the traverse studied by Villa et al. (2014) there is a spatial regularity: the lowermost grade zones in the W (the Houillère Unit) are weakly metamorphosed sediments; further ESE, in the Ruitor Unit, higher strain rates and high pressure parageneses are observed; the most high-grade zones, the Piemont-Ligurian (P-L) Oceanic Unit and the Monte Rosa nappe further east, consist of eclogites. A straightforward prediction from “closure temperature” theory is illustrated in Figure 4a: detrital ages are preserved in the low-grade metasedimentary units recording lower T than the white mica “ T_c ”, while ages steadily decrease when peak temperatures progressively exceeded “ T_c ”, being “cooling ages”. The observations presented in Figure 4b do not follow the predictions in Figure 4a. The data, however, show a regularity in the different geological units that can yield profound insight.

In the Houillère Unit (Figure 4b, blue trapezium, horizontal ruling) the Ar loss from white mica reaches 80 %, exceeding that predicted by the very low prevailing temperature conditions. In the PL Oceanic Unit and the Monte Rosa nappe (Figure 4b, green trapezium, vertical ruling) phengite ages are constant at 47 Ma and agree with garnet Lu-Hf ages. This is best explained as complete Ar retention. Muscovite ages do not decrease despite the increasing temperature, i.e. they are not “cooling ages”. Finally, in the Ruitor Unit white mica ages do decrease from W to E, but this decrease correlates with total strain and especially with the degree of phengitic substitution in the detrital muscovite (Figure 4b, purple arrow).

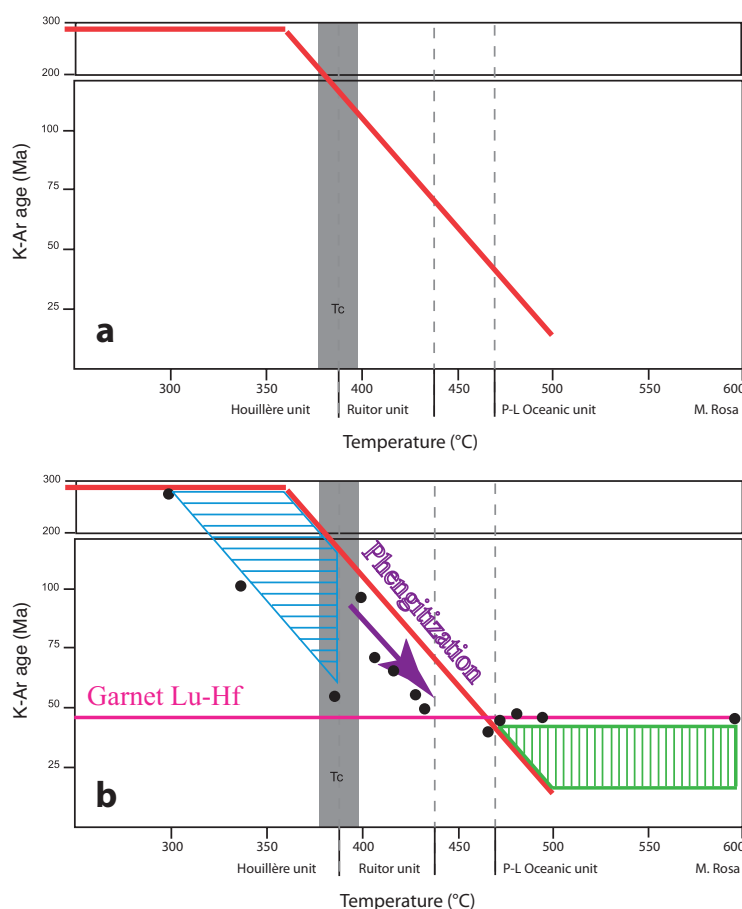


Figure 4. (a) Expected behaviour of muscovite ages in a regional metamorphic gradient following the “closure temperature” approach (red line). Detrital muscovites far to the left of the grey band indicating the “closure temperature” preserve the source age, then become younger approaching it; the age of eclogitization is found at the intersection of the red line and the grey band. Eclogitic mica samples become steadily younger, as they record post-peak “cooling ages”. The slope and the linearity of the age-distance trend are an illustration only; in the “closure temperature” approach the slope is uniquely constrained by each sample’s local exhumation rate and the trend may be concave, convex, sinusoidal, or otherwise irregular. (b) Observed mineral age pattern in the Western Alps traverse documented by Villa et al. (2014). Black dots, muscovite ^{39}Ar - ^{40}Ar ; magenta horizontal line, garnet Lu-Hf ages. Deviations of individual black dots from the red line are not random, but follow distinct patterns. Fast Ar loss in the Houillère Unit (horizontally ruled blue trapezium) at low temperature is associated to sediment dehydration, abundant aqueous fluid circulation, and abundant mica recrystallization. Slow Ar loss in the P-L Oceanic Unit and the Monte Rosa nappe (vertically ruled green trapezium) is the typical behaviour of phengite; age uniformity between mica samples, and proximity of mica ages with garnets dated by Lu-Hf (horizontal magenta line), are strong evidence that phengite accurately dates the eclogitic peak at 47 ± 1 Ma. The apparent correlation between white mica ages and temperature in the Ruitor Unit is actually a correlation between Si concentration and Ar loss (purple arrow). This means that rejuvenation is due to phengitization. Both require the recrystallization of the detritic muscovite.

Once the petrological stage is set, geochronology is straightforward. The observation that Ar can be almost completely lost at $T < 380^\circ\text{C}$ while at the same time it can almost completely be retained at $T \geq 600^\circ\text{C}$ appears initially counterintuitive if one assumes that ages are a unique function of T . The pattern in the Houillère Unit is explained by sedimentological arguments: during diagenesis, sediments are dehydrated, and large amounts of circulating water very efficiently promote recrystallization (and attendant Ar loss). In the Ruitor Unit, a similar uniform eastward age decrease is observed, which follows an apparently unrelated pattern: mica rejuvenation correlates with phengite content. In principle it could be construed that the younger phengite ages are caused by a lower “closure temperature” of phengite relative to muscovite. However, petrographic evidence requires instead that phengite *replaced* muscovite during HP metamorphism. These samples do not record progressively higher diffusive loss from one inert matrix. They record instead a progressive increase of retrogression reactions, aided by strain, which produce a heterochemical replacement mineral with associated Ar loss.

The field evidence (Figure 4b) thus features a sawtooth pattern of eastward decreasing mica ages within two separate lithological units, Houillère and Ruitor. Both patterns are imperfectly proxied by T , but are really caused by recrystallization. Occam’s razor would cut the ad-hoc assumptions that complicate the logical chain: if the correlation between the true controlling factor (recrystallization in a chemically open system) and the proxy (eastings) is not tight, why then would one resort to the proxy of a proxy, namely T representing eastward distance?

In summary, the “closure temperature” approach is unable to predict the three features that characterize the Western Alps traverse: the Ar loss at $T < 380^\circ\text{C}$, the Ar retention at $T \geq 600^\circ\text{C}$, and the tight correlation between age and phengitic substitution (blue, green, and purple

patterns in Figure 4, respectively). It should be replaced by a context-dependent, process-oriented petrological analysis.

A similar pattern had been observed by Sanchez et al. (2011), who observed that in order to date the deformation, even in cases of very high strain at relatively high T (ca. 400°C), it is necessary that an altogether new phengite phase be crystallized. When muscovite porphyroclasts are preserved as petrographic relicts, the Ar system in these minerals is not reset.

The observation that mica minerals in eclogite-facies metamorphism show a high retentivity of Ar (Di Vincenzo et al., 2001, 2004; Halama et al., 2014; Villa et al., 2014) and of radiogenic Sr (Kühn et al., 2000; Glodny et al., 2008) is not an artefact of the high-pressure conditions, which, at least in principle, could impede the removal of diffused radiogenic Ar and Sr from the intergranular space and favour their subsequent reincorporation into the mica grains. It is also observed in Barrovian polymetamorphic gneisses of the Central Alps. In a combined electron microprobe - Rb-Sr - ^{39}Ar - ^{40}Ar study, Heri et al. (2014) documented that a separated muscovite sample, originally distributed as “age standard” B4M, is composed of at least three different white mica generations (Figure 5) that coexist in mutual chemical and isotopic disequilibrium. What is most remarkable is that B4M underwent Oligocene metamorphic temperatures exceeding 600°C , yet did not achieve full diffusive equilibration, neither of major and trace elements, nor of the $^{87}\text{Sr}/^{86}\text{Sr}$ ratio, nor of the $^{40}\text{Ar}/^{40}\text{K}$ ratio.

Extrapolation of laboratory data?

One problem that underlies most geological reconstructions is that the time-scale of human observations is much shorter than that of the natural processes being observed. This forces geologists to extrapolate any laboratory data on process rates acquired over at most a few

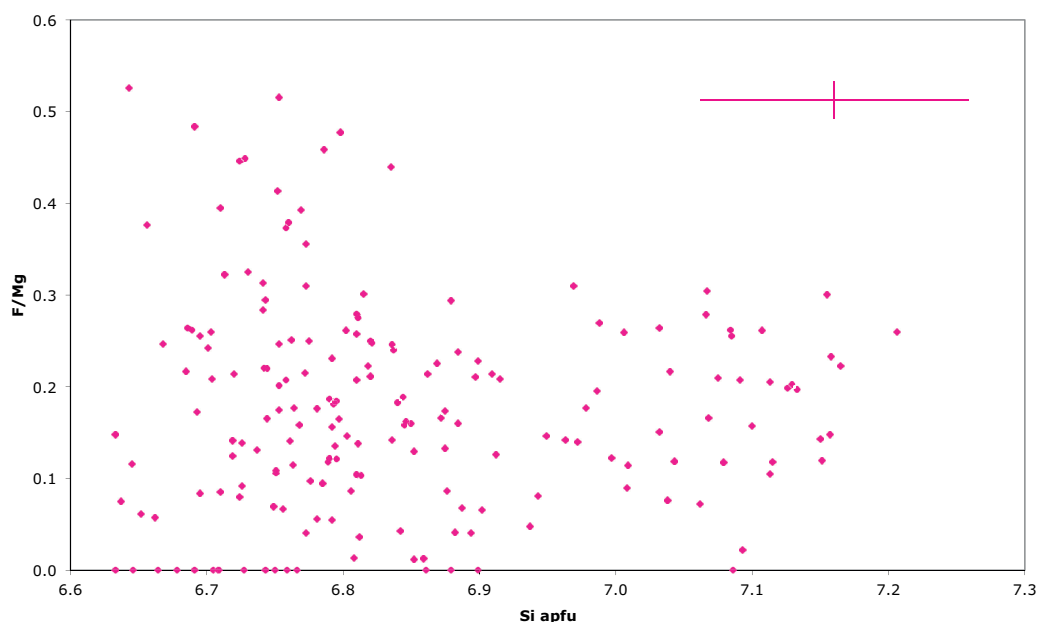


Figure 5. Electron microprobe analyses of mounted grains of the B4M muscovite “standard” (data by Heri et al., 2014). The absolute uncertainty of the abscissa is 0.1, that of the ordinate 0.02, as shown by the cross in the upper right corner. In this sample, originally separated from a gneiss, phengite ($\text{Si} \geq 7.2$ atoms per formula unit, apfu) coexists with at least two very different low-Si muscovite generations having different fluorine concentrations: one is practically halogen-free, one has a high F/Mg ratio. This rock was not equilibrated despite reaching $> 600^\circ\text{C}$ during the Oligocene. Its mineralogical diversity, i.e. petrological disequilibrium, corresponds to isotopic disequilibrium of both Ar and Sr.

weeks by several orders of magnitude. This works very well in simple physical systems, for which the mathematical equations governing the behaviour of a limited number of quantities are rigorously known. As for the geological systems, the question is to what extent the true physical mechanisms are correctly understood.

Can diffusion rates in minerals be accurately measured in laboratory experiments such that their extrapolation to geological temperatures and timescales is legitimate? The answer is yes and no. The determination of diffusion rates of divalent cations in garnet (Chakraborty and Ganguly, 1992) is one of the most elegant and successful experiments in modern petrology. Garnet is an anhydrous mineral and remains

stable under the experimental conditions reported by Chakraborty and Ganguly (1992). In contrast to garnet, mica is unstable when heated in air or in vacuum, and water must be added to the experimental capsule to stabilize it (Giletti, 1974). The presence of water, as discussed in detail by Villa (2010, p. 5-6), allows Wood-Walther dissolution, which overruns diffusion in the experimental capsule just as it does in nature. The result (Hess et al., 1987; Villa and Puxeddu, 1994) is that it has not been possible to this day to achieve control on mineral degradation during laboratory attempts to measure Ar diffusivity of hydrous phases. Accordingly, the extrapolation of laboratory experiments underestimates the true

Ar retentivity of hydrous mineral chronometers such as hornblende (Villa et al., 1996), biotite (Villa, 2010), and white mica (Villa et al., 2014). A typical example is that of biotite. The attempt to determine its diffusivity in the laboratory (Giletti, 1974) returned a “closure temperature” (radius and cooling rate as above) $T_c = 404\text{ }^{\circ}\text{C}$. However, in the classical Central Alps location biotite retained Ar 3 Ma before the rock cooled through the Paragonite-in isograd at $480\text{ }^{\circ}\text{C}$; the temperature prevailing at the time when biotite retained its Ar was between 500 and $560\text{ }^{\circ}\text{C}$ (Figure 3b). The downslope extrapolation of the tangled diffusion+dissolution rate obtained in the laboratory by Giletti (1974) has no geological relevance.

Anhydrous phases such as feldspars survive laboratory experiments apparently intact. It has thus been proposed (McDougall and Harrison, 1988) that the degassing rate of Ar in feldspar can be extrapolated from ca. 700 - $1000\text{ }^{\circ}\text{C}$ in the laboratory to ca. 200 - $300\text{ }^{\circ}\text{C}$ in natural systems.

A priori arguments based on the discontinuous deformations and vibrations of crystal structures based on quantum solid-state physics (Villa, 2006, 2014) predict that the feldspar structure is not an inert matrix as required by diffusion theory. Additionally, a monoclinic-triclinic phase transition, known to occur around $700\text{ }^{\circ}\text{C}$ when heating plagioclase from room temperature (Smith, 1974, p. 305), is associated with an anomalous Ar degassing rate (Cassata and Renne, 2013, Figure 16). When a perthitic sample is heated in the laboratory, the K-feldspar (Kfs) lamellae intergrown with the plagioclase lamellae are also passively distorted by the phase transition in plagioclase, precisely at temperatures close to those for which Arrhenian nonlinearity of the ³⁹Ar release is observed (see Villa, 2014). The laboratory data acquired above the phase transition are not expected to have any relevance for the geological history occurring at 200 - $300\text{ }^{\circ}\text{C}$. As for the data points acquired at temperatures below the

phase transition, it might seem legitimate to extrapolate them if they were monomineralic Kfs, but one must not forget the chemical phase fingerprinting provided by the Ca/Cl/K ratios. It was documented, by the convergent results of several analytical techniques (Chafe et al., 2014), that at least the archetypal microcline used to promote diffusionism in Kfs consists of a number of mineral generations visible at the μm scale, including one or more non-feldspathic alteration/retrogression phases (such as sericite, clays, etc.), feldspathic replacement products (adularia), microcline, and high-temperature plagioclase intergrowths. Each of the observed phases has its own, distinct Ar outgassing rate. The bulk sample containing a variety of phases has a composite outgassing rate resulting from the sum of the massbalance-weighted individual Ar outgassing rates of each phase. This phase mosaic, and attending systematics of the Ar outgassing, probably can be revealed in all deuterically coarsened microclines, as they record fluid interaction (Worden et al., 1990). The polymineralic nature of a Kfs sample forbids to extrapolate the data obtained in the laboratory at temperatures below that of the phase transition. If one were to attempt such extrapolation, one would first have to document (following the multi-analytical protocols of Chafe et al., 2014) that the analysed sample is strictly monomineralic. In case one such sample were found, it would then be mandatory to assess whether it verifies or falsifies the *a priori* theoretical arguments made by Villa (2014). One necessary mathematical self-consistency test using the Fechtig equations is explained in detail by Villa (2006, p. 168-170). Because of the length of the mathematical/physical technical aspects, a repetition of the procedure is out of place here. Readers who have access to a computer are strongly encouraged to duplicate the mathematical self-consistency test. Only in case that a monomineralic Kfs sample would respect the Fechtig equations (for which there

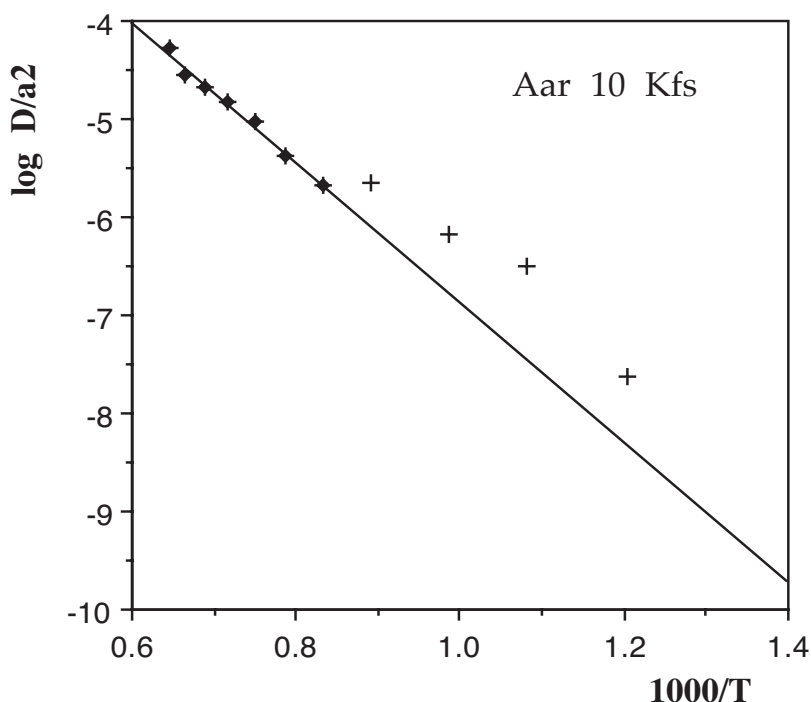


Figure 6. Arrhenius diagram of the ^{39}Ar degassing rate of Kfs Aar 10 (data by Villa and Hanchar, 2013). If the solid line fitting the seven filled circles is extrapolated to the well-constrained geologically relevant temperature of 450°C (corresponding to $x = 1.383$), an unrealistic maximum heating time of 37 a is calculated. Fitting the crosses gives an even higher diffusivity and an even more unrealistic maximum heating time. Extrapolating laboratory degassing rates to natural conditions produces inaccurate results in K-feldspar.

are no known examples to this day) one could assess the internal consistency of diffusion modelling *a posteriori*.

Most often the reconstruction of “cooling histories” is based on geochronological data interpreted as a function of T_c , so that a consistency test involves circular reasoning. Only tight non-geochronological constraints on a sample’s thermal history, which can be controlled independently, are useful for a consistency assessment. There is unfortunately an extremely small number of truly independently constrained thermal histories of Kfs: two were reviewed by Villa and Puxeddu,

1994; one by Villa, 2006; seven by Villa et al., 2006; and one follows below.

Diffusive modelling can be applied at different levels of sophistication (e.g. McDougall and Harrison, 1988). The approach making the least number of black-box assumptions is that by Harrison and Bé (1983). These authors evaluated the lowest diffusion coefficient obtained by laboratory degassing, and from that they calculated the maximum time that a Kfs sample could have spent at a given constant temperature before it was completely outgassed. Their only assumption was that the extrapolation of the laboratory degassing rate is an accurate and

faithful proxy of Ar loss at ambient temperatures of 200-300 °C over geological times.

As already pointed out by Villa (2014) and Chafe et al. (2014), recalculating randomly selected examples by the very proponents of this approach reveals internal inconsistencies. Moreover, the predicted geological diffusivities are orders of magnitude too high and heating durations are correspondingly too short. An additional example is the Aar 10 K-feldspar from an orthogneiss in the Aar Massif in the Alps (Villa and Hanchar, 2013), whose granitic protolith was intruded at *ca.* 300 Ma. The sample lies next to a small shear zone with a *ca.* 20 m offset and underwent a very well-constrained peak temperature of 450 ± 20 °C (Marquer and Burkhard, 1992; see also Rossi and Rolland, 2014). It records a staircase-shaped age spectrum ranging between 9 and 35 Ma. From the ^{39}Ar - ^{40}Ar data by Villa and Hanchar (2013) it is possible to construct an Arrhenius diagram of the ^{39}Ar release rate (Figure 6). The smallest apparent diffusivity is given by the seven high-temperature steps between 859 and 1190 °C. A weighted least squares regression of these steps gives $\text{MSWD} = 0.86$, $D_0/a^2 = (2^{+3}_{-1.4}) \text{ s}^{-1}$ and $E = (138 \pm 13) \text{ kJ/mol}$. If regression slope and intercept are interpreted as Fickian diffusion parameters, it is then possible to apply the approach by Harrison and Bé (1983) and constrain an upper limit for the time that the Kfs spent at 450 °C without losing all of the ^{40}Ar that it contained beforehand. According to the assumed initial Ar concentration of the microcline (^{40}Ar concentrations corresponding to apparent ages of 300 Ma and 35 Ma are the two extremes), the required loss during the ductile deformation at 9 Ma is between 95.6 and 50.3 %, respectively. In the assumption of Fickian diffusion both in nature and in the laboratory, the maximum time that a 300 Ma old feldspar could have survived at 450 °C without being outgassed to give a high-temperature age younger than 35 Ma is 1.17×10^9 s, or 37 a. This is a shorter duration for regional metamorphism than is possible on the basis of the

heat transfer of rocks. Even if the 450 °C were not interpreted as the regional metamorphic peak temperature and were instead viewed as heating by fault friction, this would imply that the total displacement of the fault, 20 m, was achieved in less than 37 a. This requires a minimum slip rate of 0.5 m/a, which is just as unreasonable geologically. The necessary implication is that the degassing rate at 450 °C is not accurately predicted by extrapolating downslope the degassing rate acquired in the laboratory above 859 °C.

Concluding remarks

The ^{39}Ar - ^{40}Ar technique can provide correlated information on the presence of mineral mixtures and on the ages of the phases forming the mixture. It can produce accurate results especially when it is associated with high-resolution petrography and petrology. Imaging of heterochemical mineral generations is just as important for geochronology as is mass spectrometry.

Amphiboles are stable over a broad compositional and *P-T* range, and consequently polygenetic, heterochemical mixtures are often observed in metamorphic rocks. Unravelling the ages of several coexisting amphibole generations is possible using Ca-Cl-K-Ar correlation diagrams.

The use of Ca-Cl-K-Ar correlation diagrams, supported by electron probe microanalyses, can be exported to other minerals as well. Especially white mica, biotite and K-feldspar are amenable to recognition of heterochemical mixtures. In the white mica family, resolvable differences in the Ca/K and Cl/K ratios of paragonite, phengite, margarite and muscovite were documented. In the biotite family, electron microprobe has shown that Cl/K ratios do discriminate between successive generations. In the feldspar family, microcline and adularia have very different Ca/K (and Ba/K) ratios; Cl/K ratios revealed sericitization that had escaped casual optical

microscopy. More in general, minute alteration phases are easily detected by their anomalous Ca/Cl/K signature. As in each of these examples the chemical signature was associated to an age variation, Occam's razor suggests that each heterochemical phase was assigned its age. Establishing a context between the Ca/Cl/K ratios provided by ^{39}Ar - ^{40}Ar systematics and major element ratios (Si/Al, Na/Mg, etc.) that have a petrological significance allows dating of entire segments of the P-T-A-X trajectories.

In all examples documented in detail so far (amphibole, K-feldspar, biotite and white mica) it was observed that multiple mineral generations, whenever they are preserved in a sample, are quite resilient to complete diffusive loss of Ar. This runs counter the simple down-temperature extrapolation of laboratory degassing rates.

The extremely strong preponderance of dissolution rates relative to diffusion rates imply that a small amount of water in a metamorphic environment is capable of overwhelming any diffusive loss, which is very slow *per se* in the absence of water, by effecting partial or total recrystallization. This justifies the working hypothesis that mineral geochronometers are more sensitive to water than to temperature, and behave therefore as hygrochronometers.

Acknowledgements

Reviews by J. Glodny, A.R. Heri, Y. Rolland, Xiao Long and by Guest Editor P. Fiannacca greatly helped improve the manuscript.

References

- Allaz J., Berger A., Engi M. and Villa I.M. (2011) - The effects of retrograde reactions and of diffusion on ^{39}Ar - ^{40}Ar ages of micas. *Journal of Petrology*, 52, 691-716.
- Cassata W.S. and Renne P.R. (2013) - Systematic variations of argon diffusion in feldspars and implications for thermochronometry. *Geochimica et Cosmochimica Acta*, 112, 251-287.
- Chafe A.N., Villa I.M., Hanchar J.M. and Wirth R. (2014) - A re-examination of petrogenesis and $^{40}\text{Ar}/^{39}\text{Ar}$ systematics in the Chain of Ponds K-feldspar: "diffusion domain" archetype versus polyphase hygrochronology. *Contributions to Mineralogy and Petrology*, 167(5), paper 1010, 1-17.
- Cherniak D.J., Hanchar J.M. and Watson E.B. (1997) - Rare earth diffusion in zircon. *Chemical Geology*, 134, 289-301.
- Cherniak D.J., Watson E.B., Grove M. and Harrison T.M. (2004) - Pb diffusion in monazite: a combined RBS/SIMS study. *Geochimica et Cosmochimica Acta*, 68, 829-840.
- Chakraborty S. and Ganguly J. (1992) - Cation diffusion in aluminosilicate garnets: experimental determination in spessartine \pm almandine diffusion couples, evaluation of effective binary diffusion coefficients, and applications. *Contributions to Mineralogy and Petrology*, 111, 74-86.
- Di Vincenzo G., Ghiribelli B., Giorgetti G. and Palmeri R. (2001) - Evidence of a close link between petrology and isotope records; constraints from SEM, EMP, TEM and in situ ^{40}Ar - ^{39}Ar laser analyses on multiple generations of white micas (Lanternman Range, Antarctica). *Earth and Planetary Science Letters*, 192, 389-405.
- Di Vincenzo G., Carosi R. and Palmeri R. (2004) - The relationship between tectono-metamorphic evolution and argon isotope records in white mica: constraints from in situ ^{40}Ar - ^{39}Ar laser analysis of the variscan basement. *Journal of Petrology*, 45, 1013-1043.
- Dodson M.H. (1973) - Closure temperature in cooling geochronological and petrological systems. *Contributions to Mineralogy and Petrology*, 40, 259-274.
- Gebauer D., Quadf A.v., Compston W., Williams I.S. and Grünenfelder M. (1988) - Archean zircons in a retrograded Caledonian eclogite of the Gotthard massif (Central Alps, Switzerland). *Schweizerische Mineralogische und Petrographische Mitteilungen*, 68, 485-490.

- Giletti, B.J. (1974) - Studies in diffusion I: argon in phlogopite mica. In: Hofmann, A.W., Giletti, B.J., Yoder, H.S. and Yund, R.A. (eds), *Geochemical transport and kinetics. Carnegie Institution of Washington Publication*, 634, 107-115.
- Glodny J., Kuhn A. and Austrheim H. (2008) - Diffusion versus recrystallization processes in Rb-Sr geochronology: isotopic relics in eclogite facies rocks, Western Gneiss region, Norway. *Geochimica et Cosmochimica Acta*, 72, 506-525.
- Halama R., Konrad-Schmolke M., Sudo M., Marshall H.R. and Wiedenbeck M. (2014) - Effects of fluid-rock interaction on $^{40}\text{Ar}/^{39}\text{Ar}$ geochronology in high-pressure rocks (Sesia-Lanzo Zone, Western Alps). *Geochimica et Cosmochimica Acta*, 126, 475-494.
- Harrison T. and Bé K. (1983) - $^{40}\text{Ar}/^{39}\text{Ar}$ age spectrum analysis of detrital microclines from the southern San Joaquin Basin, California: an approach to determining the thermal evolution of sedimentary basins. *Earth and Planetary Science Letters*, 64, 244-256.
- Hart S.R. (1964) - The petrology and isotopic-mineral age relations of a contact zone in the Front Range, Colorado. *Journal of Geology*, 72, 493-525.
- Heri A.R., Robyr M. and Villa I.M. (2014) - Petrology and geochronology of the "muscovite standard" B4M. In: Jourdan F., Mark D. and Verati C. (eds.) $^{40}\text{Ar}/^{39}\text{Ar}$ Dating: from Geochronology to Thermochronology, from Archaeology to Planetary Sciences. *Geological Society London Special Publications*, 378, 69-78.
- Hess J.C., Lippolt H.J. and Wirth R. (1987) - Interpretation of $^{40}\text{Ar}/^{39}\text{Ar}$ spectra of biotites - evidence from hydrothermal degassing experiments and TEM studies. *Chemical Geology*, 66, 137-149.
- Jamtveit B. (2010) - Metamorphism: from patterns to processes. *Elements*, 6, 149-152.
- Janots E., Engi M., Berger A., Allaz J. and Schwarz O. (2008) - Prograde metamorphic sequence of REE minerals in pelitic rocks of the Central Alps: implications for allanite-monazite-xenotime phase relations from 250 to 610 °C. *Journal of Metamorphic Geology*, 26, 509-526.
- Janots E., Engi M., Rubatto D., Berger A., Gregory C. and Rahn M.K. (2009) - Metamorphic rates in collisional orogeny from in situ allanite and monazite dating. *Geology*, 37, 11-14.
- Kühn A., Glodny J., Iden K. and Austrheim H. (2000) - Retention of Precambrian Rb/Sr ages through Caledonian eclogite facies metamorphism, Bergen Arc Complex, W-Norway. *Lithos*, 51, 305-330.
- Lasaga A.C. and Rye D.M. (1993) - Fluid flow and chemical reaction kinetics in metamorphic systems. *American Journal of Science*, 293, 361-404.
- Marquer D. and Burkhard M. (1992) - Fluid circulation, progressive deformation and mass-transfer processes in the upper crust; the example of basement-cover relationships in the External Crystalline Massifs, Switzerland. *Journal of Structural Geology*, 14, 1047-1057.
- McDougall I. and Harrison T. (1988) - Geochronology and thermochronology by the $^{40}\text{Ar}/^{39}\text{Ar}$ method. Oxford University Press, New York, 212 pp.
- Putnis A. and Austrheim H. (2013) - Mechanisms of metasomatism and metamorphism on the local mineral scale: The role of Dissolution-Reprecipitation during mineral re-equilibration. In: Harlov D.E., Austrheim H. (eds.), *Metasomatism and the Chemical Transformation of Rock*. Springer, Heidelberg, 141-170. ISBN 978-3-642-28393-2.
- Rossi M. and Rolland Y. (2014) - Stable isotope and Ar/Ar evidence of prolonged multiscale fluid flow during exhumation of orogenic crust: Example from the Mont Blanc and Aar Massifs (NW Alps). *Tectonics*, 33, 1681-1709.
- Sanchez G., Rolland Y., Schneider J., Corsini M., Olliot E., Goncalves P., Verati C., Lardeaux J.-M. and Marquer D. (2011) - Dating low-temperature deformation by $^{40}\text{Ar}/^{39}\text{Ar}$ on white mica, insights from the Argentera-Mercantour Massif (SW Alps). *Lithos*, 125, 521-536.
- Smith J.V. (1974) - *Feldspar Minerals*. Springer, Heidelberg, Vol. I.
- Steck A. and Hunziker J. (1994) - The tertiary structural and thermal evolution of the Central Alps - compressional and extensional structures in an orogenic belt. *Tectonophysics*, 238, 229-254.
- Tartèse R., Ruffet G., Poujol M., Boulvais P. and Ireland T.R. (2011) - Simultaneous resetting of the muscovite

- K-Ar and monazite U-Pb geochronometers: a story of fluids. *Terra Nova*, 23, 390-398.
- Tilton G.R. (1960) - Volume diffusion as a mechanism for discordant lead ages. *Journal of Geophysical Research*, 65, 2933-2945.
- Villa I.M. (1998) - Isotopic closure. *Terra Nova*, 10, 42-47.
- Villa I.M. (2001) - Radiogenic isotopes in fluid inclusions. *Lithos*, 55, 115-124.
- Villa I.M. (2006) - From the nm to the Mm: isotopes, atomic-scale processes, and continent-scale tectonic models. *Lithos*, 87, 155-173.
- Villa I.M. (2010) - Disequilibrium Textures vs Equilibrium Modelling: Geochronology at the Crossroads. In: Spalla M.I., Marotta A.M. and Gosso G. (eds) Advances in interpretation of geological processes. *Geological Society London Special Publications*, 332, 1-15.
- Villa I.M. (2014) - Ar diffusion in K-feldspar: present and absent. In: Jourdan F., Mark D. and Verati C. (eds.) $^{40}\text{Ar}/^{39}\text{Ar}$ Dating: from Geochronology to Thermochronology, from Archaeology to Planetary Sciences. Geological Society London Special Publications, 378, 107-116.
- Villa I.M. and Hanchar J.M. (2013) - K-feldspar hygrochronology. *Geochimica et Cosmochimica Acta*, 101, 24-33.
- Villa I.M. and Puxeddu M. (1994) - Geochronology of the Larderello geothermal field: new data and the "closure temperature" issue. *Contributions to Mineralogy and Petrology*, 115, 415-426.
- Villa I.M. and Williams M.L. (2013) - Geochronology of metasomatic events. In: Harlov D.E. and Austrheim H. (eds.), Metasomatism and the Chemical Transformation of Rock. Springer, Heidelberg, 171-202. ISBN 978-3-642-28393-2.
- Villa I.M., Grob  y B., Kelley S.P., Trigila R. and Wieler R. (1996) - Assessing Ar transport paths and mechanisms for McClure Mountains Hornblende. *Contributions to Mineralogy and Petrology*, 126, 67-80.
- Villa I.M., Hermann J., M  ntener O. and Trommsdorff V. (2000) - ^{39}Ar - ^{40}Ar dating of multiply zoned amphibole generations (Malenco, Italian Alps). *Contributions to Mineralogy and Petrology*, 140, 363-381.
- Villa I.M., Ruggieri G. and Puxeddu M. (2001) - Geochronology of magmatic and hydrothermal micas from the Larderello geothermal field. In: R. Cidu (Ed.), Water-Rock interaction 10. Balkema, Lisse (NL), 1589-1592.
- Villa I.M., Ruggieri G., Puxeddu M. and Bertini G. (2006) - Geochronology and isotope transport systematics in a subsurface granite from the Larderello-Travale geothermal system (Italy). *Journal of Volcanology and Geothermal Research*, 152, 20-50.
- Villa I.M., Bucher S., Bousquet R., Kleinhanns I.C. and Schmid S.M. (2014) - Dating polygenetic metamorphic assemblages along a transect through the Western Alps. *Journal of Petrology*, 55, 803-830.
- Wetherill G.W. (1963) - Discordant Uranium-Lead Ages 2. *Journal of Geophysical Research*, 68, 2957-2965.
- Wood B.J. and Walther J.V. (1983) - Rates of hydrothermal reactions. *Science*, 222, 413-415.
- Worden R.H., Walker F.D.L., Parsons I. and Brown W.L. (1990) - Development of microporosity, diffusion channels and deuteric coarsening in perthitic alkali feldspars. *Contributions to Mineralogy and Petrology*, 104, 507-515.

Submitted, March 2015 - Accepted, September 2015